Closed-form solutions of spinning, eccentric binary black holes at 1.5 post-Newtonian order

Rickmoy Samanta ●,[1,2] Sashwat Tanay ●,[3,4,*] and Leo C. Stein[4]

[1]*Indian Statistical Institute, 203 B. T. Road, Kolkata 700108, India*
[2]*Birla Institute of Technology and Science Pilani, Hyderabad 500078, India*
[3]*Laboratoire Univers et Théories, Observatoire de Paris,*
Université PSL, Université Paris Cité, CNRS, F-92190 Meudon, France
[4]*Department of Physics and Astronomy, The University of Mississippi, University, Mississippi 38677, USA*

The closed-form solution of the 1.5 post-Newtonian (PN) accurate binary black hole (BBH) Hamiltonian system has proven to be evasive for a long time since the introduction of the system in 1966. Solutions of the PN BBH systems with arbitrary parameters (masses, spins, eccentricity) are required for modeling the gravitational waves emitted by them. Accurate models of gravitational waves are crucial for their detection by LIGO/Virgo and LISA. Only recently, two solution methods for solving the BBH dynamics were proposed in Ref. [G. Cho and H. M. Lee, Phys. Rev. D **100**, 044046 (2019)] (without using action-angle variables), and Refs. [S. Tanay *et al.*, Phys. Rev. D **103**, 064066 (2021), S. Tanay *et al.*, Phys. Rev. D **107**, 103040 (2023)] (action-angle based). This paper combines the ideas laid out in the above articles, fills the missing gaps and compiles the two solutions which are fully 1.5PN accurate. We also present a public *Mathematica* package BBHPNTOOLKIT which implements these two solutions and compares them with the result of numerical integration of the evolution equations. The level of agreement between these solutions provides a numerical verification for all the five action variables constructed in Refs. [S. Tanay *et al.*, Phys. Rev. D **103**, 064066 (2021), S. Tanay *et al.*, Phys. Rev. D **107**, 103040 (2023)]. This paper hence serves as a stepping stone for pushing the action-angle-based solution to 2PN order via canonical perturbation theory.

I. INTRODUCTION

Construction of accurate gravitational wave (GW) templates (or models) has been crucial to the GW detections that have taken place so far since 2015 [1–3]. This is so because the method of matched filtering for GW detection requires as one of the inputs, the theoretical templates of the GW signal to be detected. Post-Newtonian (PN) theory serves as a useful framework within which GWs from binary black holes (BBHs) are modeled when the system is in its initial and longest-lived inspiral stage [4]. At this stage, the two black holes (BHs) of the BBH are far apart and move slowly around a common center. This is also referred to as the PN regime. In the PN framework, quantities of interest are presented in a PN power series in the small PN paramter (ratio of the typical speed of the system and that of light). As is typical of power series, higher-order corrections are of smaller magnitudes and carry higher PN orders. Since GWs from a BBH are functions of the positions momenta of the source, modeling the positions momenta of the BBH system is crucial for constructing the GW templates. This paper deals with the construction of 1.5PN accurate closed-form solutions of the BBH system.

Since we restrict ourselves to 1.5PN order, the dissipative effects on the BBH dynamics due to GW emission do not enter the picture; they show up at 2.5PN. The conservative dynamics of the system can be described with the PN Hamiltonian framework, wherein the system possesses a Hamiltonian that is a function of the system's canonical coordinates [5]. The leading PN order effect is simply that of two point masses moving under mutual Newtonian gravitational attraction whose Hamiltonian treatment is a textbook subject matter. Such systems, move on a closed ellipse if they are bound. The next level of sophistication is at 1PN order wherein 1PN effects are added to the above Newtonian system. At this level, spin effects are ignored (they enter at 1.5PN). Reference [6] provided the quasi-Keplerian parametric solution for this system; the trajectory is no longer a closed ellipse and the system features the advance of periastron. The orbit still remains confined in a plane due to the constancy of the angular momentum vector.

Moving further up the PN ladder, we encounter the 1.5PN system whose Hamiltonian was proposed in Ref. [7]. At 1.5PN order, spin effects come into play for the first time via a spin-orbit interaction (linear in spin), while the spin-spin

*sashwat.tanay@obspm.fr

interaction terms enter at 2PN. Via numerical integration of the resulting equations of motion (EOMs), it is seen that the orbital plane precesses; the orbital angular momentum is constant only in magnitude, but not in direction. This system displays the rich interplay of nonzero BH spins, periastron precession, along with spin and orbital-plane precession. We concern ourselves with this system in this paper.

Over the past decades, solutions to the dynamics of the spinning BBH system (at 1.5PN order or higher) have been constructed by many groups [8–16], but most of them worked under some simplifying specialization like only one BH spinning, equal masses, small eccentricity, orbit-averaging, etc. Two recent breakthroughs have occurred on the front of finding solutions to the most general 1.5PN BBH system without any simplifying assumptions where the qualifier "most general" indicates a system with arbitrary values of masses, spins, and eccentricity, while still falling under the PN regime.[1] The first breakthrough was made by Cho and Lee in Ref. [17] where they succeeded in integrating the EOMs of the system; the 1PN term in the Hamiltonian was ignored throughout for simplicity. The second breakthrough came in the form of Refs. [18,19], where the authors evaluated all the action variables [actions as in action-angle (AA) variables] and laid out a scheme on how to construct the AA-based solution of the system.[2] Against this backdrop, this paper aims to target the following objectives

(1) Represent the solution of Ref. [17] but with the 1PN terms included. We will call it the standard solution.

(2) Present a systematic procedure to construct the AA-based solution. As we will see later, the construction of the AA-based solution requires the standard solution as one of the inputs.

(3) Make available BBHPNTOOLKIT, a public *Mathematica* package [21] that (1) implements the standard solution, the AA-based solution, and the numerical solution (2) gives the numerical values of all five frequencies (rate of increase of the angle variables) of a given BBH system, (3) computes the Poisson brackets (PBs) between any two functions of the phase-space variables.

Let us mention that the AA-based solution provides a significant advantage over the standard solution. This is so because while extending the standard solution to 2PN appears quite difficult, the AA-based solution should be extendable to 2PN via canonical perturbation theory. This paper assembles the ideas put forth in Refs. [18,19,22], and provides a solid platform from where one can springboard

to push the 1.5PN solutions to 2PN order using canonical perturbation theory.

The organization of the paper is as follows. In Sec. II, we introduce the phase space, the Hamiltonian, the EOMs of the system as well as the concept of AA variables. In Sec. III, we represent the solution of Ref. [22] with the 1PN terms included (standard solution). In Sec. IV, we lay out an in a step-by-step fashion, the strategy to construct the alternative AA-based solution. In Sec. V, we introduce the *Mathematica* package BBHPNTOOLKIT that we release with this paper. We also make comparisons of our analytical solutions with the numerical one, before summarizing in Sec. VI.

II. THE SETUP

This paper is the culmination of the research initiated in Refs. [17–19]. Since the notations and conventions used in the first article differs from those in the other two articles, the notations and conventions of this paper are a mix of the two types.

The system in consideration is a BBH system in the PN approximation. It consists of two BHs of masses m_1 and m_2 such that the relative separation vector of the first BH from the second one is $\vec{R}$. We choose to work in the center-of-mass frame throughout wherein the momenta of the first BH is equal to the negative of the other and is represented by $\vec{P}$. The total angular momenta of the BBH system is $\vec{J} = \vec{L} + \vec{S}_1 + \vec{S}_2$, where $\vec{L} \equiv \vec{R} \times \vec{P}$, and $\vec{S}_1$ and $\vec{S}_2$ are the spin angular momenta of the two BHs. We also define the total mass $M = m_1 + m_2$, the reduced mass $\mu \equiv m_1 m_2 / M$, the symmetric mass ratio $\nu \equiv \mu / M$, and $\sigma_1 \equiv 1 + 3m_2/4m_1$ and $\sigma_2 \equiv 1 + 3m_1/4m_2$, along with

$$\vec{S}_{\text{eff}} \equiv \sigma_1 \vec{S}_1 + \sigma_2 \vec{S}_2. \tag{1}$$

As usual, G and c denote the gravitational constant and the speed of light, respectively. Finally, note that we represent the physical time with t', whereas $t \equiv t'/(GM)$ is reserved for the scaled time. Dots represent a derivative taken with respect to t. The norm of any 3D vector will be denoted by the same letter as the vector but without the arrow, i.e., $V \equiv |\vec{V}|$. The unit vector $\vec{V}/V$ corresponding to a vector $\vec{V}$ is denoted by the use of a hat $\hat{V} \equiv \vec{V}/V$.

We now present the 1.5PN Hamiltonian of the system using scaled variables $\vec{r} \equiv \vec{R}/(GM)$, $\vec{p} \equiv \vec{P}/\mu$,

$$H = H_{\text{N}} + H_{\text{1PN}} + H_{\text{1.5PN}} + \mathcal{O}(c^{-4}), \tag{2}$$

where the various PN components are

$$H_{\text{N}} = \mu \left(\frac{p^2}{2} - \frac{1}{r} \right), \tag{3}$$

---

[1]In the PN approximation, the spin magnitude of a maximally spinning BH is 0.5PN order smaller than the BH's orbital angular momentum.

[2]See Ref. [20] for a pedagogical introduction to the action-angle method of solution.

$$H_{\text{1PN}} = \frac{\mu}{c^2} \left\{ \frac{1}{8}(3\nu - 1)p^4 + \frac{1}{2r^2} \right. \tag{4}$$

$$\left. - \frac{1}{2r}[(3 + \nu)p^2 + \nu(\hat{r} \cdot \vec{p})^2] \right\}, \tag{5}$$

$$H_{\text{1.5PN}} = \frac{2G}{c^2 R^3} \vec{S}_{\text{eff}} \cdot \vec{L}. \tag{6}$$

The evolution of any function g is given by its Poisson bracket (PB) with H

$$\frac{dg}{dt'} = \{g, H\}. \tag{7}$$

A few basic rules are needed to evaluate the PB between any two functions of the phase space variables $\vec{R}, \vec{P}, \vec{S}_1$, and $\vec{S}_2$, the first one being the PB between the phase space variables. The only nonvanishing PBs between the phase-space variables are given by

$$\{R^i, P_j\} = \delta^i_j, \quad \text{and} \quad \{S^i_a, S^j_b\} = \delta_{ab}\epsilon^{ij}_k S^k_a, \tag{8}$$

and those related by the property of antisymmetry of the PBs

$$\{f, g\} = -\{g, f\}. \tag{9}$$

a, b have been used to label the BHs, whereas i, j, k label the components of the vectors. ϵ^{ij}_k is the usual Levi-Civita symbol in three dimensions. This is despite the appearance of lower index k, whose sole purpose is to implement Einstein summation. The second rule is the so-called chain rule (with v_ls standing for the phase-space variables)

$$\{f, g(v_l)\} = \{f, v_l\}\frac{\partial g}{\partial v_l}. \tag{10}$$

Finally, with the aid of Eqs. (8), (9), and (10), we can evaluate the PB between any two quantities. This also lets us evaluate the time derivative of any quantity via Eq. (7).

Two quantities f and g are said to commute or be in involution if $\{f, g\} = 0$. A system with Hamiltonian H in $2n$ canonical momenta-positions coordinates $(\vec{\mathcal{P}}, \vec{\mathcal{Q}})$ is said to be integrable if there exists a canonical transformation to new momenta-positions coordinates $(\vec{\mathcal{J}}, \vec{\theta})$ such that H is a function of only the $\mathcal{J}$s, and that all the $\vec{\mathcal{P}}$ and $\vec{\mathcal{Q}}$ are 2π-periodic functions of the angle variables $\vec{\theta}$ [23]. An integrable system possesses n mutually commuting constants, including the Hamiltonian (Liouville-Arnold theorem). Another equivalent but practically more useful definition of actions is given via [23,24]

$$\mathcal{J}_k = \frac{1}{2\pi}\oint_{\mathcal{C}_k} \Theta = \frac{1}{2\pi}\oint_{\mathcal{C}_k} \mathcal{P}_i d\mathcal{Q}^i, \tag{11}$$

where $\mathcal{C}_k$ is any loop in the kth homotopy class on the n torus defined by the constant values of the n commuting constants.

Before ending this section, we will touch upon the concept of flows under a function f of the phase-space variables and the associated vector fields. $f(\vec{\mathcal{P}}, \vec{\mathcal{Q}})$ defines a vector field as $\{\cdot, f\} = \partial/\partial\lambda$, and its action on another function $g(\vec{\mathcal{P}}, \vec{\mathcal{Q}})$ is $\partial g/\partial\lambda = \{g, f\}$ [25]. The integral curves of the vector field is referred to as the flow of the field. With this, it is easy to see that the equation governing the real-time evolution of a Hamiltonian system $dg/dt' = \{g, H\}$ is basically the flow equation under the Hamiltonian where the flow parameter λ is to be taken as time t'. The next two sections deal with two equivalent ways of constructing the solution of 1.5PN BBH system.

III. THE STANDARD SOLUTION

The standard solution is constructed by integrating the flow equations under the 1.5PN Hamiltonian. Reference [17] constructed the solution of the 1.5PN BBH system but omitted the 1PN term of the Hamiltonian entirely in their analysis as it was deemed by the authors to be simple to deal with. Here we include the 1PN terms too. Most of the derivation in Ref. [17] goes through, even after including the 1PN terms. So, we closely follow their approach and do not present the entire derivation. We provide derivation details only for those segments where the derivation presented in Ref. [17] has to be significantly modified due to the inclusion of the 1PN terms. Needless to say, we refer the reader to Ref. [17] for the derivation of many of the results that we present in this section. Reference [17] also has some typos that we fix in this paper.

A. Angles between the $\vec{L}$, $\vec{S}_1$, and $\vec{S}_2$

We introduce scaled variables via $\vec{l} \equiv \vec{L}/(\mu GM)$, $h \equiv H/\mu$, and $\vec{s}_a \equiv \vec{S}_a/(\mu GM)$, where $a = 1, 2$ serve to distinguish the two BHs. Let κ_1, κ_2, and γ denote the angle between the vector pairs $(\vec{L}, \vec{S}_1)$, $(\vec{L}, \vec{S}_2)$, and $(\vec{S}_1, \vec{S}_2)$. Without loss of generality, we assume that $m_1 > m_2$. Under the 1.5PN Hamiltonian, L, S_1, and S_2 remain constant in time as their PB with the Hamiltonian vanishes.

The solution for $\cos\kappa_1$ and its method of derivation is the same as that presented in Sec. III A of Ref. [17], which was done without including the 1PN term in the Hamiltonian. Here we directly present that solution. It reads

$$\cos\kappa_1(t) = x_1 + (x_2 - x_1)\text{sn}^2(\Upsilon(t), \beta). \tag{12}$$

The quantities used in the above equation are defined below. x_1, x_2, x_3 are the roots of the following cubic equation (in the order $x_1 < x_2 < x_3$[3])

$$- 2\delta_1 L S_1 (\delta_1 - \delta_2) x^3 - [L^2 (\delta_1 - \delta_2)^2 + 2\delta_2 L \Sigma_2 S_2 (\delta_2 - \delta_1)$$
$$+ \delta_1^2 S_1^2 + 2\delta_1 \delta_2 \Sigma_1 S_1 S_2 + \delta_2^2 S_2^2] x^2 + 2\delta_2 S_2 [L \Sigma_1 (\delta_2 - \delta_1)$$
$$+ \Sigma_2 (\delta_1 S_1 + \delta_2 \Sigma_1 S_2)] x - \delta_2^2 S_2^2 (\Sigma_1^2 + \Sigma_2^2 - 1) = 0. \quad (13)$$

Σ_1, Σ_2, δ_1, and δ_2 are constant quantities defined as

$$\Sigma_1 \equiv \frac{\vec{S}_1 \cdot \vec{S}_2}{S_1 S_2} - \frac{L}{S_2} \frac{\delta_1 - \delta_2}{\delta_2} \frac{\vec{L} \cdot \vec{S}_1}{L S_1}, \quad (14)$$

$$\Sigma_2 \equiv \frac{\vec{L} \cdot \vec{S}_2}{L S_2} + \frac{\delta_1 S_1}{\delta_2 S_2} \frac{\vec{L} \cdot \vec{S}_1}{L S_1}, \quad (15)$$

$$\delta_a \equiv 2\nu\sigma_a, \qquad (a = 1, 2). \quad (16)$$

It is easy to rewrite Σs in terms of other constants of motion as [see Eqs. (A8) and (A9) of Ref. [19]]

$$\Sigma_1 = \frac{\sigma_2 (J^2 - L^2 - S_1^2 - S_2^2) - 2 S_{\text{eff}} \cdot L}{2\sigma_2 S_1 S_2}, \quad (17)$$

$$\Sigma_2 = \frac{S_{\text{eff}} \cdot L}{\sigma_2 L S_2}, \quad (18)$$

which goes on to show that the Σs are also constants of motion. We still need more description to fully explicate the solution given in Eq. (12).

$$\Upsilon(t) = \frac{\sqrt{A(x_3 - x_1)}}{2} \left(\alpha + \frac{v + e \sin v}{c^2 l^3} \right), \quad (19)$$

$$\beta = \sqrt{\frac{x_2 - x_1}{x_3 - x_1}}, \quad (20)$$

$$\alpha = \frac{\pm 2}{\sqrt{A(x_3 - x_1)}} F \left(\arcsin \sqrt{\frac{\cos\kappa_1(t=0) - x_1}{x_2 - x_1}}, \beta \right), \quad (21)$$

$$A = 2 l s_1 \delta_1 (\delta_2 - \delta_1), \quad (22)$$

$$v = 2 \arctan \left(\sqrt{\frac{1 + e}{1 - e}} \tan \frac{u}{2} \right), \quad \text{or} \quad (23)$$

$$= u + 2 \arctan \left(\frac{\beta_e \sin u}{1 - \beta_e \cos u} \right), \quad (24)$$

$$\beta_e = \frac{e}{1 + (1 - e^2)^{1/2}}, \quad (25)$$

$$n(t - t_0) = u - e \sin u, \quad (26)$$

$$n = (-2h)^{3/2}, \quad (27)$$

$$e = \sqrt{1 + 2hl^2}, \quad (28)$$

$$F(\phi_p, k) \equiv \int_0^{\phi_p} \frac{d\theta}{\sqrt{1 - k^2 \sin^2 \theta}}, \quad (29)$$

$$\text{sn}(F, k) \equiv \sin(\text{am}(F, k)) \equiv \sin\phi_p. \quad (30)$$

Note that Eqs. (23), (26), (27), and (28) give the true anomaly, Kepler equation, mean motion and the eccentricity, respectively, all at the Newtonian level. Also, it is important to mention that Eq. (24) is preferred over Eq. (23) because its rhs does not have the discontinuity due to arctan, the way the rhs of Eq. (23) has. This renders the latter not so useful beyond the timespan of one orbital period. In Eqs. (29) and (30), F is the incomplete elliptic integral of the first kind, whereas sn and am are the Jacobi sin and amplitude functions, respectively. Finally, the $+$ sign in Eq. (21) is chosen if $d\cos\kappa_1/dt > 0$ at initial time, otherwise we choose the $-$ sign.

The cosine of the other two remaining angles κ_2 and γ between the various angular momenta can be easily had from the solution for $\cos\kappa_1$ [given in Eq. (12)], supplemented by Eqs. (14) and (15). This finally leads to

$$\cos\gamma = \Sigma_1 + \frac{L}{S_2} \frac{\delta_1 - \delta_2}{\delta_2} \cos\kappa_1, \quad (31)$$

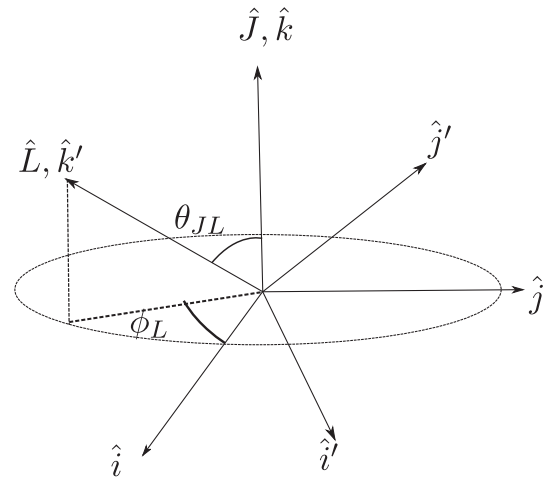$$\cos\kappa_2 = \Sigma_2 - \frac{\delta_1 S_1}{\delta_2 S_2} \cos\kappa_1. \quad (32)$$

FIG. 1. The noninertial $(i' j' k')$ frame (centered around $\hat{L} \equiv \vec{L}/L$) is displayed along with the inertial (ijk) frame (centered around $\hat{J} \equiv \vec{J}/J$).

---

[3]Reference [17] uses a different ordering of the roots $x_2 < x_3 < x_1$.

B. Solution for $\vec{L}$

For the solution of $\vec{L}$, we will use an inertial frame (call it IF), whose z axis is aligned with $\vec{J}$; see Fig. 1. In this frame, $\vec{L}$ has a polar angle θ_L and an azimuthal angle ϕ_L. Because $dL/dt = 0$, we need to determine only these two angles to determine $\vec{L}$. Since

$$\cos\theta_L = \frac{\vec{L}\cdot\vec{J}}{LJ} = \frac{L^2 + LS_1\cos\kappa_1 + LS_2\cos\kappa_2}{LJ}, \tag{33}$$

this means that we can construct $\cos\theta_L$ as a function of time from our already-constructed solutions for the cosines of κ_1, κ_2, and γ in Sec. III A.

The solution for the azimuthal angle ϕ_L of $\vec{L}$ in the IF and its method of derivation closely follows Sec. III B of Ref. [17]. So without presenting the derivation, we again directly present the solution which reads

$$\phi_L(t) - \phi_{L_0} = \mathcal{F}(t), \tag{34}$$

where the function $\mathcal{F}(t)$ is

$$\mathcal{F}(t) = \frac{2}{\sqrt{A(x_3 - x_1)}} \left(\frac{\beta_1 \Pi(\frac{x_1-x_2}{\alpha_1+x_1}, \mathrm{am}(\Upsilon,\beta),\beta)}{\alpha_1 + x_1} - \frac{\beta_2 \Pi(\frac{x_1-x_2}{\alpha_2+x_1}, \mathrm{am}(\Upsilon,\beta),\beta)}{\alpha_2 + x_1} \right), \tag{35}$$

with

$$\alpha_1 = -\frac{\delta_2(j + l + s_2\sigma_2)}{s_1(\delta_1 - \delta_2)}, \tag{36}$$

$$\alpha_2 = -\frac{\delta_2(-j + l + s_2\sigma_2)}{s_1(\delta_1 - \delta_2)}, \tag{37}$$

$$\beta_1 = -\delta_2 \frac{l^2\delta_1 + j^2\delta_2 + s_1(\delta_1 - \delta_2)(s_1 + s_2\sigma_1) + ls_2\delta_1\sigma_2 + j[l(\delta_1 + \delta_2) + s_2\sigma_2\delta_2]}{2s_1(\delta_1 - \delta_2)}, \tag{38}$$

$$\beta_2 = -\delta_2 \frac{l^2\delta_1 + j^2\delta_2 + s_1(\delta_1 - \delta_2)(s_1 + s_2\sigma_1) + ls_2\delta_1\sigma_2 - j[l(\delta_1 + \delta_2) + s_2\sigma_2\delta_2]}{2s_1(\delta_1 - \delta_2)}. \tag{39}$$

ϕ_{L_0} is an integration constant to be determined by substituting $t = 0$ in Eq. (34).[4]

C. Solution for $\vec{S}_1$ and $\vec{S}_2$

In Ref. [17], the full solution of $\vec{S}_1$ was not presented in the same way as for $\vec{L}$. However, we can construct the solution for $\vec{S}_1$ in a way that parallels very closely the method that Ref. [17] adopted to construct the solution of $\vec{L}$.[5] So, again we merely present the solution without derivation.

Just like $\vec{L}$, $\vec{S}_1$ is described by its polar and azimuthal angles (θ_{S1} and ϕ_{S1}, respectively) because its magnitude is fixed. For the polar angle, we have just like before

$$\cos\theta_{S1} = \frac{\vec{S}_1\cdot\vec{J}}{S_1 J} = \frac{S_1^2 + \vec{L}\cdot\vec{S}_1 + \vec{S}_1\cdot\vec{S}_2}{S_1 J},$$
$$= \frac{S_1^2 + LS_1\cos\kappa_1 + S_1S_2\cos\gamma}{S_1 J}, \tag{40}$$

which means that $\cos\theta_{S1}$ can be had from our previously constructed solutions of cosines of κ_1, κ_2, and γ.

The solution for the azimuthal angle $\phi_{S1}(t)$ of $\vec{S}_1$ in the IF is given by

$$\phi_{S_1}(t) - \phi_{S_{10}} = \mathcal{G}(t), \tag{41}$$

where the function $\mathcal{G}(t)$ is

---

[4]The corresponding equations in Ref. [17] [Eqs. (3.28)] have typos.

[5]$\vec{L}$ solution was constructed in Ref. [17] by introducing an "$\vec{L}$-centered" noninertial frame, whose z axis was aligned with $\vec{L}$. To construct the $\vec{S}_1$ solution using this method, we need to introduce an "$\vec{S}_1$-centered" noninertial frame whose z axis is aligned with $\vec{S}_1$.

$$\mathcal{G}(t) = \frac{2}{\sqrt{A(x_3 - x_1)}} \left(\frac{\beta_{1s1} \Pi(\frac{x_1 - x_2}{\alpha_{1s1} + x_1}, \mathrm{am}(\Upsilon, \beta), \beta)}{\alpha_{1s1} + x_1} - \frac{\beta_{2s1} \Pi(\frac{x_1 - x_2}{\alpha_{2s1} + x_1}, \mathrm{am}(\Upsilon, \beta), \beta)}{\alpha_{2s1} + x_1} \right) + \frac{v + e \sin v}{c^2 l^3} j\delta_2, \qquad (42)$$

with

$$\alpha_{1s1} = \frac{\delta_2(-j + s_1 + s_2\sigma_1)}{l\delta_1}, \qquad (43)$$

$$\alpha_{2s1} = \frac{\delta_2(j + s_1 + s_2\sigma_1)}{l\delta_1}, \qquad (44)$$

$$\beta_{1s1} = -\delta_2 \frac{l^2\delta_1 + (s_1(\delta_1 - \delta_2) + j\delta_2)(-j + s_1 + s_2\sigma_1) + ls_2\delta_1\sigma_2}{2l\delta_1}, \qquad (45)$$

$$\beta_{2s1} = \delta_2 \frac{-l^2\delta_1 + (-s_1\delta_1 + (j + s_1)\delta_2)(j + s_1 + s_2\sigma_1) - ls_2\delta_1\sigma_2}{2l\delta_1}. \qquad (46)$$

ϕ_{S_10} is an integration constant to be determined by substituting $t = 0$ in Eq. (41). This completes the solution for $\vec{S}_1$. Now $\vec{S}_2$ can also be easily had from

$$\vec{S}_2 = \vec{J} - \vec{L} - \vec{S}_1. \qquad (47)$$

D. Solution for $\vec{R}$

Specification of $\vec{R}$ can be broken down into its magnitude R and its azimuthal angle (phase) ϕ in a precessing plane that is perpendicular to $\vec{L}$. The solution for $\vec{R}$ proceeds along the same lines as in Ref. [17], but is somewhat modified due to the inclusion of the 1PN term in the Hamiltonian. So, unlike previous subsections, we will present the derivation of the solution for ϕ. Since the magnitude of $\vec{R}$ has already been worked out in the literature, we will simply state the relevant results without presenting the derivation.

Let us first focus on the magnitude r of the scaled position vector $\vec{r} = \vec{R}/(GM)$. The 1PN and 2PN contributions (without spins) can be found in Ref. [6], whereas the 1.5PN contribution (with the 1PN effects ignored) can be found in Ref. [26]. Combining these results together, we have up to 1.5PN order the following quasi-Keplerian parametric solution for r

$$r = a_r(1 - e_r \cos u),$$
$$l' \equiv n(t - t_0) = u - e_t \sin u, \qquad (48)$$

with u and l' standing for the eccentric and the mean anomalies, respectively. The other constants that comprise the above solution are

$$a_r = -\frac{1}{2h}\left(1 - \frac{1}{2}(\nu - 7)\frac{h}{c^2} - 2\frac{s_{\mathrm{eff}} \cdot l}{l^2}\frac{h}{c^2}\right), \qquad (49)$$

$$e_r^2 = 1 + 2hl^2 - 2(6 - \nu)\frac{h}{c^2} - 5(3 - \nu)\frac{h^2 l^2}{c^2}$$
$$+ 8(1 + hl^2)\frac{s_{\mathrm{eff}} \cdot l}{l^2}\frac{h}{c^2}, \qquad (50)$$

$$n = (-2h)^{3/2}\left(1 + \frac{2h}{8c^2}(15 - \nu)\right), \qquad (51)$$

$$e_t^2 = 1 + 2hl^2 + 4(1 - \nu)\frac{h}{c^2} + (17 - 7\nu)\frac{h^2 l^2}{c^2}$$
$$+ 4\frac{s_{\mathrm{eff}} \cdot l}{l^2}\frac{h}{c^2}, \qquad (52)$$

where the following definitions have been used

$$\vec{s}_{\mathrm{eff}} \equiv \delta_1\vec{s}_1 + \delta_2\vec{s}_2, \qquad (53)$$

$$s_{\mathrm{eff}} \cdot l \equiv \vec{s}_{\mathrm{eff}} \cdot \vec{l}. \qquad (54)$$

Recall that $s_{\mathrm{eff}} \cdot l$ is a constant since its PB with H vanishes. This definition, along with Eq. (1) implies the following relation

$$\vec{s}_{\mathrm{eff}} \equiv \frac{2}{GM^2}\vec{S}_{\mathrm{eff}}. \qquad (55)$$

With the magnitude of $\vec{r}$ being taken care of, we can now move on to determine its phase in a plane perpendicular to $\vec{l}$. The scaled-time derivative (with respect to t) of the scaled position vector $\vec{r}$ is

$$\frac{d\vec{r}}{dt} = \{\vec{r}, H\}, \qquad (56)$$
$$= \vec{p} + \frac{1}{2c^2 r^3}(-2\nu(\vec{p} \cdot \vec{r})\vec{r} - (6 + 2\nu)r^2\vec{p}$$
$$+ (3\nu - 1)p^2 r^3\vec{p} - 2\vec{r} \times \vec{s}_{\mathrm{eff}}), \qquad (57)$$

which when solved perturbatively gives the following expression for $\vec{p}$

$$\vec{p} = \frac{d\vec{r}}{dt} + \frac{1}{c^2}\left(\frac{\vec{r} \times \vec{s}_{\rm eff} + \nu(\vec{p} \cdot \vec{r})\vec{r}}{r^3}\right.$$
$$\left. + \frac{d\vec{r}}{dt}\left(\frac{p^2}{2} - \frac{3p^2\nu}{2} + \frac{3+\nu}{r}\right)\right). \qquad (58)$$

At this point, we introduce a noninertial frame (call it NIF) whose x, y, and z axes are along $\vec{J} \times \vec{L}, \vec{L} \times (\vec{J} \times \vec{L})$, and $\vec{L}$, respectively. The Euler matrix which when multiplied with a column consisting of a vector's components in the IF, gives its components in the NIF is

$$E_L = \begin{pmatrix} -\sin\phi_L & \cos\phi_L & 0 \\ -\cos\theta_L\cos\phi_L & -\cos\theta_L\sin\phi_L & \sin\theta_L \\ \cos\phi_L\sin\theta_L & \sin\theta_L\sin\phi_L & \cos\theta_L \end{pmatrix}. \qquad (59)$$

In the NIF, the various vector components are

$$\vec{l} = \begin{bmatrix} 0 \\ 0 \\ l \end{bmatrix}_n, \qquad (60)$$

$$\vec{s}_1 = s_1 \begin{bmatrix} \sin\kappa_1\cos\xi \\ \sin\kappa_1\sin\xi \\ \cos\kappa_1 \end{bmatrix}_n, \qquad (61)$$

$$\vec{s}_2 = s_2 \begin{bmatrix} \sin\kappa_2\cos(\xi+\psi) \\ \sin\kappa_2\sin(\xi+\psi) \\ \cos\kappa_2 \end{bmatrix}_n, \qquad (62)$$

$$\vec{r} = \begin{bmatrix} r\cos\phi \\ r\sin\phi \\ 0 \end{bmatrix}_n. \qquad (63)$$

Note that with the aid of Eqs. (61) and (62), we have actually defined the angles ξ and ψ, that is to say, ξ and $\xi + \psi$ are azimuthal angles of $\vec{s}_1$ and $\vec{s}_2$ in the NIF. Implicit in Eq. (63) is the definition that ϕ is the azimuthal angle of $\vec{r}$ in the NIF. Also, the subscript "n" after the above columns denotes that the components have been written in the NIF.

Being cognizant of the fact that the time derivative of a vector changes (as a geometrical object) with a change of the frame in which it is viewed (see Sec. 4.9 of Ref. [27]), we mention here that all time derivatives of vectors in this paper are to be viewed in the IF. With that, we now wish to express the components of $d\vec{r}/dt$ in the NIF. We do so by first writing the $\vec{r}$ components in the IF [using Eq. (63) and the inverse of E_L of Eq. (59)], taking derivatives of the components with respect to t, and then transforming the components of this time derivative to the NIF (using E_L). The end result is

$$\dot{\vec{r}} = \begin{bmatrix} \dot{r}\cos\phi - r\sin\phi(\dot{\phi}_L\cos\theta_L + \dot{\phi}) \\ \dot{r}\sin\phi + r\cos\phi(\dot{\phi}_L\cos\theta_L + \dot{\phi}) \\ r(-\dot{\phi}_L\sin\theta_L\cos\phi + \dot{\theta}_L\sin\phi) \end{bmatrix}_n. \qquad (64)$$

Now we want to express $\vec{l} = \vec{r} \times \vec{p}$ in component form in the NIF. The components of $\vec{l}$ and $\vec{r}$ in the NIF are already given by Eqs. (60) and (63). For $\vec{p}$, we start with Eq. (58), where we use Eqs. (61) and (62) for expressing $\vec{s}_{\rm eff}$, and Eq. (64) for $d\vec{r}/dt$. With all this, the third component of the relation $\vec{l} = \vec{r} \times \vec{p}$ when written out gives us (with $\epsilon \equiv 1/c^2$ and $h \equiv H/\mu$)

$$\frac{d\phi}{dt} = -\frac{2(\epsilon s_1\delta_1\cos\kappa_1 + \epsilon s_2\delta_2\cos\kappa_2 + lr)}{r^2(-2\epsilon(3+\nu) + (-2 + \epsilon(-1+3\nu))((\vec{p}\cdot\hat{r})^2 + \frac{l^2}{r^2}))r)} - \cos\theta_L\frac{d\phi_L}{dt}. \qquad (65)$$

We mention that to arrive at Eq. (65) we eliminated p^2 in favor of $\vec{p} \cdot \hat{r}$ (or $\vec{p} \cdot \vec{r}$) with the aid of

$$p^2 = (\vec{p}\cdot\hat{r})^2 + \frac{l^2}{r^2}, \qquad (66)$$

where $\vec{p} \cdot \hat{r}$ is given by [see Eq. (36) of Ref. [18]]

$$\vec{p} \cdot \hat{r} = \left((2h - \epsilon(3\nu - 1)h^2) + \frac{2(1 + \epsilon(4-\nu)h)}{r} + \frac{(-l^2 + \epsilon(6+\nu))}{r^2} + \frac{-\epsilon\nu(l^2 + 2s_{\rm eff} \cdot l/\nu)}{r^3}\right)^{1/2}. \qquad (67)$$

We want to rewrite Eq. (65) so that the only time-varying quantities on the rhs are $\cos\kappa_1$ and r. Therefore, we need to eliminate $\vec{p} \cdot \hat{r}, d\phi_L/dt, \cos\theta_L$, and $\cos\kappa_2$. To do so, we make use of Eqs. (32), (67) and the relations

$$\vec{L} \cdot \vec{J} = JL\cos\theta_L = \vec{L} \cdot (\vec{L} + \vec{S}_1 + \vec{S}_2) = L^2 + LS_1\cos\kappa_1 + LS_2\cos\kappa_2, \qquad (68)$$

$$\frac{d\phi_L}{dt} = \frac{1}{c^2 r^3} \left(\frac{\beta_1}{\cos\kappa_1 + \alpha_1} - \frac{\beta_2}{\cos\kappa_1 + \alpha_2} \right). \tag{69}$$

Equation (69) has already been derived in Ref. [17], see its Eq. (3.27). Finally, Eq. (65) becomes

$$\frac{d\phi}{dt} = \frac{\epsilon}{r^3} \left(\frac{\beta_1}{\cos\kappa_1 + \alpha_1} + \frac{\beta_2}{\cos\kappa_1 + \alpha_2} \right) - \frac{l\epsilon^2(-1 + 3\nu)(2s_{\text{eff}} \cdot l + l^2\nu)}{2r^5} + \frac{l\epsilon^2(-6 + 17\nu + 3\nu^2)}{2r^4}$$
$$+ \frac{l(2 - h^2\epsilon^2(1 - 3\nu)^2 + 2h\epsilon(-1 + 3\nu))}{2r^2} - \frac{\epsilon(-s_{\text{eff}} \cdot l + l^2(4 + 4h\epsilon - 2\nu - 13h\epsilon\nu + 3h\epsilon\nu^2 + \delta_1 + \delta_2) + ls_2\delta_2\Sigma_2)}{lr^3}, \tag{70}$$

$$\equiv \frac{\epsilon}{r^3} \left(\frac{\beta_1}{\cos\kappa_1 + \alpha_1} + \frac{\beta_2}{\cos\kappa_1 + \alpha_2} \right) + \frac{A_5}{r^5} + \frac{A_4}{r^4} + \frac{A_3}{r^3} + \frac{A_2}{r^2}, \tag{71}$$

which when integrated gives

$$\phi - \phi_0 = \frac{2}{\sqrt{A(x_3 - x_1)}} \left(\frac{\beta_1 \Pi(\frac{x_1 - x_2}{\alpha_1 + x_1}, \text{am}(\Upsilon, \beta), \beta)}{\alpha_1 + x_1} \right.$$
$$\left. + \frac{\beta_2 \Pi(\frac{x_1 - x_2}{\alpha_2 + x_1}, \text{am}(\Upsilon, \beta), \beta)}{\alpha_2 + x_1} \right) + A_5\mathcal{R}_5$$
$$+ A_4\mathcal{R}_4 + A_3\mathcal{R}_3 + A_2\mathcal{R}_2, \tag{72}$$

where ϕ_0 is an integration constant to be determined by substituting $t = 0$ in the above equation. Note that Eq. (71) defines A_2, A_3, A_4, and A_5. Also, $\mathcal{R}_j$ is the indefinite integral of r^{-j} with respect to t. For brevity, we do not write out $\mathcal{R}_j$s explicitly but they can be easily had from the Newtonian-accurate expressions

$$r = a(1 - e\cos u), \tag{73}$$

$$l' \equiv n(t - t_0) = u - e\sin u. \tag{74}$$

n and e are given in Eqs. (28) and (27), respectively. a is the Newtonian version of the rhs of Eq. (49). Note that we have kept more than necessary PN accuracy in Eq. (70) and by extension, Eq. (72) just for the purposes of illustration; any additive term containing ϵ^q with $q \geq 2$ can be dropped.

E. Solution for $\vec{P}$

We present the determination of $\vec{P} = \mu\vec{p}$ in a step-by-step algorithmic fashion

(1) From Eqs. (66) and (67), determine p^2 or p, which takes care of the magnitude of $\vec{p}$. With this, we also have in our hands the value of $\vec{p} \cdot \hat{r}$, which will be used in the next step. What now remains is to determine the azimuthal angle of $\vec{p}$ in the NIF.

(2) Next we compute the angle ϕ_{offset}, which is defined as

$$\phi_{\text{offset}} = \arcsin \frac{L(t)}{r(t)p(t)} \quad \text{if } \vec{p} \cdot \hat{r} > 0,$$
$$\phi_{\text{offset}} = \pi - \arcsin \frac{L(t)}{r(t)p(t)} \quad \text{if } \vec{p} \cdot \hat{r} < 0. \tag{75}$$

(3) Now it is a simple matter to see that the azimuthal angle that $\vec{p}$ makes with the x axis of the NIF is $\phi + \phi_{\text{offset}}$, where ϕ is the azimuthal angle of $\vec{r}$ in the NIF and ϕ_{offset} is the relative azimuthal angle between $\vec{r}$ and $\vec{p}$. This completes the specification of $\vec{P}$.

IV. ACTION-ANGLE BASED SOLUTION

We devote this section to explaining our construction of an alternate AA-based solution to the 1.5PN BBH system. We will present in a step-by-step algorithmic fashion.

(1) The phase space of the 1.5PN system is 10-dimensional (since spin magnitudes are constants) and has five mutually commuting constants, resulting in an integrable system. These constants are $\vec{\mathcal{C}} = \{J, J_z, L, H, S_{\text{eff}} \cdot L\}$. We thus have five action variables $\vec{\mathcal{J}} = \{\mathcal{J}_1 = J, \mathcal{J}_2 = J_z, \mathcal{J}_3 = L, \mathcal{J}_4, \mathcal{J}_5\}$, which can be found in Refs. [18,19]; their notations and definitions are somewhat different from those in this paper.[6]

(2) Under the real-time evolution of the BBH system, the angles change as $\Delta\theta_i = \omega_i t'$, $t' = tGM$ being the physical time; ω_is are naturally called the frequencies of the system and are constants since they are functions of the action variables, which are themselves constants. Section VI A of Ref. [19]

---

[6]$\mathcal{J}_4$ was obtained by using Damour and Schäfer's PN extension of the Sommerfeld radial action complex contour integral [28], whereas $\mathcal{J}_5$ was obtained using the method of fictitious phase-space variables [19].

shows how to compute the five frequencies. The process mainly consists of constructing the Jacobian matrix of the actions with respect to the commuting constants, inverting this Jacobian matrix, and the row corresponding to the Hamiltonian (one of the commuting constants) contains the five frequencies.

(3) Let all the phase space variables be collectively denoted by $\vec{V} = \{\vec{R}, \vec{P}, \vec{S}_1, \vec{S}_2\}$ with their initial values being $\vec{V}_0 \equiv \vec{V}(t' = 0)$. Suppose that $\vec{V}_0$ represents the state of the system at $t' = 0$, and we want to obtain $\vec{V}(t')$ at any nonzero time t'.

(4) At $t' = 0$, assign all the angle variables of the system to have the value equal to 0: $\vec{\theta}(t' = 0) = \vec{0}$. Then at the final time t', the angles of the system would have become $\vec{\theta} = \vec{\omega} \times t'$. The problem of finding the state of the system at t' now becomes that of increasing all the angle variables by $\vec{\omega} \times t'$.

(5) As shown in Sec. VI B of Ref. [19], the angle θ_i can be increased by a certain amount if we flow under the corresponding action $\mathcal{J}_i$ by the same amount. Therefore the problem becomes that of flowing under the actions $\mathcal{J}_i$ by amounts $\omega_i t'$ (starting from the $\vec{V}_0$ configuration). The order of flows does not matter because just like all the members of $\vec{C}$, all the actions mutually commute among themselves too.

(6) Because the flow equation under the actions reads

$$\frac{d\vec{V}}{d\lambda} = \{\vec{V}, \mathcal{J}_i(\vec{C})\} = \{\vec{V}, C_j\}\frac{\partial \mathcal{J}_i}{\partial C_j}, \quad (76)$$

a flow under an action $\mathcal{J}_i$ by $\Delta\lambda_i$ can be achieved by flowing under all the commuting constants C_js by respective amounts $(\partial\mathcal{J}_i/\partial C_j)\Delta\lambda_i$. Again, we can flow under the commuting constants C_js in any order, since they all mutually commute. This finally breaks down our problem to that of flowing under all five C_js by certain amounts, whose closed-form solution is discussed in Appendix A.

Now it should be clear as to why one of the inputs to the AA-based solution is the standard solution that was presented in Sec. III. This is so because one of the commuting constants is the Hamiltonian itself and in Sec. III, we presented the solution of the flow under this commuting constant. This also happens to be the solution of the system since the system's evolution equations are same as the equations governing the flow under the Hamiltonian. Nevertheless, the AA-based solutions appears to have the advantage to be pushed to 2PN using canonical perturbation theory, which is a perturbation technique designed around the action-angle framework [27].

V. SOFTWARE PACKAGE AND COMPARISON OF THE SOLUTIONS

With this article, we are releasing a public *Mathematica* package BBHPNTOOLKIT, which accomplishes the following objectives [21]:

(1) Implements the standard solution of Sec. III obtained by integrating the flow under the Hamiltonian.

(2) Implements the action-angle-based solution of Sec. IV.

(3) Provides the numerical solution of the system by numerically integrating the EOMs.

(4) Provides numerical values of all five frequencies of the system, wherein by frequency we refer to the rates of change of the five angles (as in action-angle variables) of the system.

For the reference of the future users of our *Mathematica* package, we mention herein that we have retained some unnecessary high PN terms in the coded expressions which implement the two analytical solutions in the package. The full account is given in Appendix B. We devote this section to investigating the PN accuracy of the two analytical solutions with respect to the one got by direct numerical integration of the EOMs. In this section, we will refer to both these two analytical solutions collectively as just "analytical solutions," for these two analytical solutions agree with each much better than they do with the numerical one.

We first begin by displaying the plots of the analytical solutions along with the numerical one in Fig. 2. Plots corresponding to the two analytical solutions (standard and AA-based solutions) cannot be distinguished visually. But they are collectively distinguishable from the numerical solution at late times. As displayed in the caption of this figure, the parameters taken for these plots do not correspond to astrophysically relevant systems. But this is not a cause of concern because our focus in this section is to explore the mathematical accuracy of our solutions that are valid for a wide set of parameters and not just those which correspond to real astrophysical scenarios. Later in this section, we will see that it is actually helpful to study these solutions under nonphysical scenarios (such as changing the value of $\epsilon \equiv 1/c^2$), to determine the PN accuracy of our solutions (via the method of linear fit between the error and the PN parameter).

Let us now switch to a more technical task of determining the PN accuracy of our analytical solutions against the numerical one. We explain our comparison method with the aid of Fig. 3. Starting from $t' = t_0 = 0$, we evolve the system numerically up to a certain time $t' = t_1$, such that $\vec{R}_n$ ($\vec{R}$ got via numerical integration) differs by a small amount from $\vec{R}_a$ ($\vec{R}$ got from the analytical solution). By "small amount," we mean an opening angle (ζ_3 in Fig. 3) of ~0.5° to 1° between $\vec{R}_a$ and $\vec{R}_n$. The dashed circle in the figure
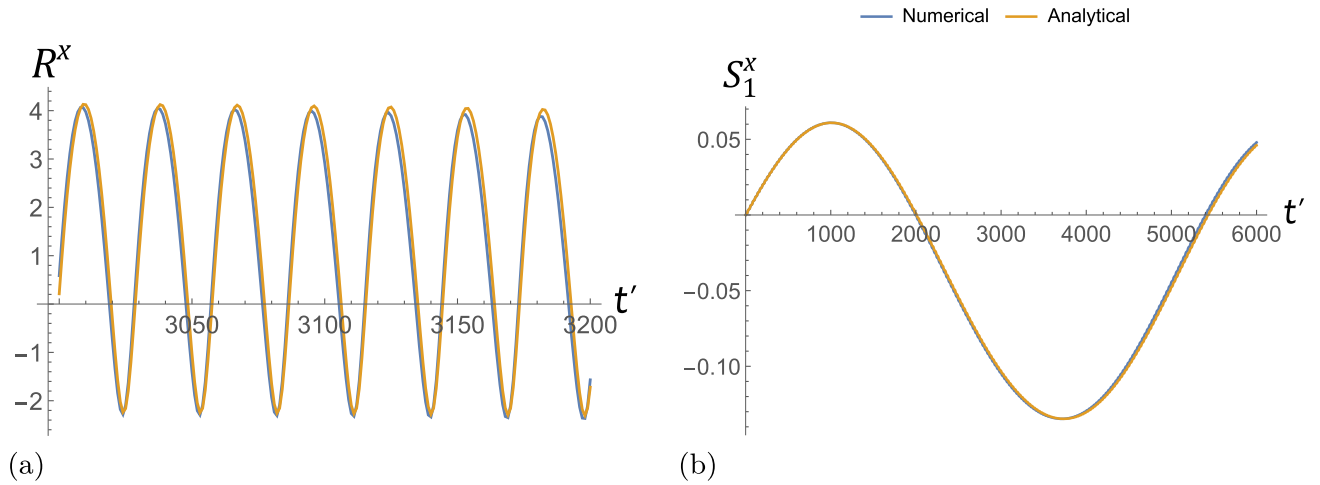
FIG. 2. Comparison of the analytical solutions with the numerical one. For a system with $(m_1, m_2) = (5/2, 1)$ and the initial values of the phase-space variables being $\vec{R} = (2, 2, 2)$, $\vec{P} = (1/2, -1/2, 1/3)$, $\vec{S_1} = \sqrt{\epsilon}\,(0, 1, 1)$, $\vec{S_2} = \sqrt{\epsilon}\,(1, -3/10, 0)$. Panels (a) and (b) show evolution of x component of $\vec{R}$ and $\vec{S_1}$, respectively. We choose $\epsilon = 0.003$ for (a) and $\epsilon = 0.01$ for (b). All this results in a Newtonian-orbital time period of $T_N \sim 29$ for both (a) and (b), and the PN parameter ~ 0.0036 for (a) ~ 0.012 for (b), respectively. Throughout we keep $G = 1$.
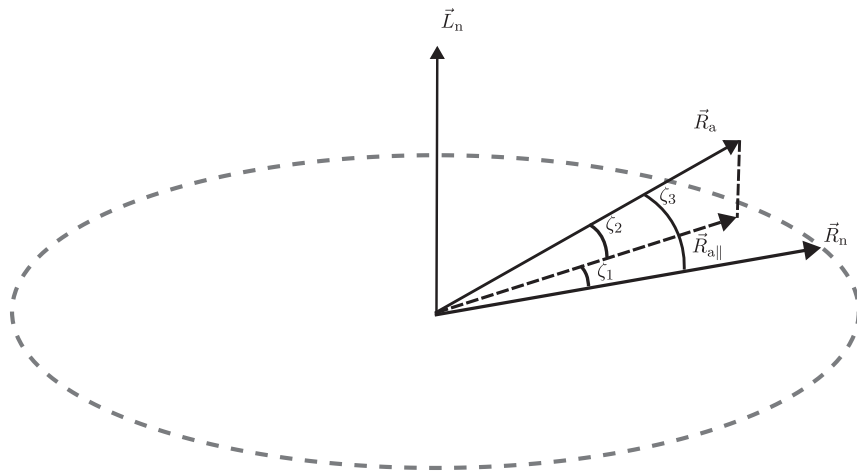

FIG. 3. Difference between the numerical and analytical position vector $\vec{R}$ being split in two perpendicular components.

denotes the plane perpendicular to $\vec{L}_n$ ($\vec{L}$ got via numerical integration at $t' = t_1$). $\vec{R}_{a\parallel}$ is the projection of $\vec{R}_a$ on this plane. The difference between $\vec{R}_n$ and $\vec{R}_a$ is greatly exaggerated in this figure for the purposes of illustration. Now, even if we ignore the numerical roundoff errors, we expect $\vec{R}_a \neq \vec{R}_n$ because of the PN truncation errors that crept in while deriving the analytical solutions. For this section, we force the roundoff errors to be much smaller than the truncation errors by keeping sufficient numerical precision while constructing the numerical solution.

Now, the $\vec{R}_a - \vec{R}_n$ can be broken down into two components: an in-plane component $\vec{R}_{a\parallel} - \vec{R}_n$, and an out-of-plane component $\vec{R}_a - \vec{R}_{a\parallel}$. The in-plane difference is brought about by an in-plane (perpendicular to $\vec{L}$)

dephasing which occurs due to the difference between the numerical and the analytical values of the mean motion n (a kind of frequency). The out-of-plane difference is brought about by the difference $\vec{L}_a - \vec{L}_n$, where $\vec{L}_a$ is the analytical $\vec{L}$.

For comparison purposes, it is convenient to think of the in-plane and out-of-plane differences as in-plane and out-of-plane dephasings happening due to a difference in some angular velocities $d\omega_\parallel$ and $d\omega_\perp$ in the two directions, with the former being essentially the difference between the analytical and numerical mean motions. As is suggested from Eq. (51), these frequencies are often expressible as a PN series. Hence, we schematically write the difference between the numerical and analytical frequencies as a PN series along the two directions as

$$d\omega_\parallel = \xi^p d\omega_{\parallel p} + \xi^{p+1} d\omega_{\parallel p+1} + \mathcal{O}(\xi^{p+2}), \quad (77)$$

$$d\omega_\perp = \xi^q d\omega_{\perp q} + \xi^{q+1} d\omega_{\perp q+1} + \mathcal{O}(\xi^{q+2}), \quad (78)$$

with ξ standing for the PN parameter $GM/(c^2 R)$. The above equations indicate that the differences in the frequencies along the two directions occurs at PN orders p and q. Note that, unlike earlier sections, p does not stand for the magnitude of the scaled momentum but is rather a PN power-counting index. It then follows that

$$|\vec{R}_{a\parallel} - \vec{R}_n| = \xi^p R_n d\omega_{\parallel p} t_1, \quad (79)$$

$$|\vec{R}_{a\parallel} - \vec{R}_a| = \xi^q R_n d\omega_{\perp q} t_1, \quad (80)$$

where the lhs is the small arc length that subtends an angle $\xi^p d\omega_{\parallel p} t_1$ or $\xi^p d\omega_{\perp p} t_1$ a distance R_n away. Adding the vectors $\vec{R}_n - \vec{R}_{a\parallel}$ and $\vec{R}_{a\parallel} - \vec{R}_a$ and taking the modulus of the sum, with the aid of the above two equations gives us at leading order

$$|\vec{R}_n - \vec{R}_a| = \xi^r t_1 R_n d\omega_{\parallel r} \quad \text{if } p \neq q, \quad (81)$$

$$= \xi^r t_1 R_n (d\omega_{\parallel p}^2 + d\omega_{\perp p}^2)^{1/2} \quad \text{if } p = q, \quad (82)$$

where $r = \min(p, q)$,[7] which is not to be confused with $r \equiv |\vec{r}|$. This finally leads to

$$\log\left(\frac{|\vec{R}_n - \vec{R}_a|}{t_1 R_n}\right) = r \log \xi + \text{constant.} \quad (83)$$

In Eq. (82), use has been made of Pythagoras theorem since $\vec{R}_n - \vec{R}_{a\parallel}$ is perpendicular to $\vec{R}_{a\parallel} - \vec{R}_a$ and $\vec{R}_n - \vec{R}_a$ forms the hypotenuse.

Equation (83) is the key to testing the PN accuracy of our analytical solutions against the numerical one. It says that a linear fit between the two logarithms has a slope equal to the integer r. From Eqs. (77) and (78), we know that r is also the PN order at which our analytical solution starts to diverge from the numerical one, if one focuses their attention on the frequencies associated with the dephashings. In our numerical experiments with a handful of cases, we find $r = 2 \pm 2.5\%$, which indicates that the analytical solutions (both kinds) deviate from the numerical one at 2PN order, as far as the combined (in-plane and out-of-plane) dephasing effect goes. To perform the linear fit associated with Eq. (83), we needed the values of the PN parameter ξ. We simply used $\xi = GM/(c^2\langle R \rangle)$, where $\langle R \rangle$ is the numerical orbit-averaged value of R.

_____

[7]Here $\min(p, q) \equiv p$ if $p < q$, and $\min(p, q) \equiv p$ if $p = q$.

Another way to compare the analytical solutions with the numerical one is to compare the timescale T_N of variation of the Newtonian orbit against timescale T_D at which $\vec{R}_n - \vec{R}_a$ varies. Assuming a relation of the form

$$T_N = \xi^r T_D, \quad (84)$$

our objective is to determine r. The above equation gives

$$\log T_D = -r \log \xi + \log T_N. \quad (85)$$

A linear fit between $\log T_D$ and $\log \xi$ gives us a slope of $-r$. For the purposes of linear fitting, we can approximate T_D as

$$T_D = \frac{2\pi t_1}{\arccos \hat{R}_n \cdot \hat{R}_a}, \quad (86)$$

and ξ is to be approximated the same way as before. This linear fit again gave us $r = 2 \pm 2.5\%$, which means that the analytical and the numerical solutions differ at 2PN order. We finally mention that the verification of the solutions presented here also serves as a verification for the five action variables constructed in Refs. [18,19].

There is a subtle aspect of the above procedure of determining the PN accuracy of the analytical solutions, which needs further elaboration. A question arises: how to vary the PN parameter $\xi \equiv GM/(c^2 R)$ to prepare the data for linear-fitting as per Eqs. (83) and (85)? We put forth two options: (1) Vary the average value of R (physically sensible) (2) Vary $\epsilon = 1/c^2$ (unphysical). We will argue below that the latter option, though unphysical, is the mathematically sound option and the former is not.

The multiplicative factors attached to powers of ξ in Eqs. (77) and (78) are assumed to depend on quantities like energy, mass ratio etc. This comes from our previous experience of the PN literature; for example see the expression of the mean motion in Eqs. (51) or (28b) of Ref. [29]. So this means that care must be taken while selecting the sample BBH systems for performing the above linear fits so that all the systems which are supposed to fall on a straight line have almost the same energy and mass ratio. One way to achieve this is to vary c, while keeping other parameters like m_1, m_2, and average R almost constant. Doing so does vary ξ. Another way to vary ξ would be to vary the masses or the average R. Doing so would also change the energy and the mass ratio in general, which is something we want to avoid. The unphysical aspect of varying the speed of light is of no concern to us as far as checking the PN accuracy of the analytical solutions is concerned. This is so because our solutions to the BBH system are valid for any arbitrary positive speeds of light, provided $\xi \ll 1$.

VI. SUMMARY

With this paper, we conclude the old problem of solving the dynamics of the 1.5PN BBH system, whose Hamiltonian was introduced in Ref. [7]. This is done for arbitrary masses, spins and eccentricity, and without any averaging. First we re-presented the solution of Ref. [22] but for completeness, unlike Ref. [22], we included the 1PN effects too. Then we show how to construct the alternative AA-based solution in an algorithmic style. The construction of the latter solution requires former solution as one of the inputs. But the AA-based solution is superior in the sense that it can be extended to 2PN order via canonical perturbation theory, with relative ease. We finally introduce BBHPNTOOLKIT, a *Mathematica* package, which implements our solutions for practical use. We finally make comparison of the two analytical solutions against the numerical one employing linear regression, and the analytical solutions indeed appear to be 1.5PN accurate.

The theoretical ideas that form the foundations of the two analytical solutions have been presented in Refs. [18,19,22]. Here we have assembled them, filled in the gaps (missing 1PN effects in Ref. [22]), implemented the solutions in a public *Mathematica* package, thereby establishing a platform (both in theoretical and practical-implementation sense) from where we can aim to push these solutions to 2PN. Moreover, the agreement between the numerical and AA-based solution serves as a nontrivial check of all the five actions constructed in Refs. [18,19].

The next natural line of action would be to extend our AA-based solution to 2PN order using canonical perturbation theory. On a parallel track, one can try to construct GWs for these systems now that their dynamics have been solved. Adding the 2.5PN dissipative effects due to radiation reaction to our analytic solution will also be an interesting endeavor for the future.

ACKNOWLEDGMENTS

APPENDIX A: SOLUTION FOR FLOW UNDER COMMUTING CONSTANTS

1. Solution for flow under H

The solution of flow under H has been constructed in Sec. III. It is mainly contained in Eqs. (12), (34), (41), (47), (72), and (75).

2. Solution for flow under $S_{\text{eff}} \cdot L$

The solution of flow under $S_{\text{eff}} \cdot L$ has been constructed in Ref. [19]; it is mainly contained in Eqs. (A39), (A66), (A76), and (A102) of that article. These four equations seem to determine only $\vec{R}, \vec{L}$, and $\vec{S}_1$, and not $\vec{S}_2$ and $\vec{P}$. But once we have $\vec{R}, \vec{L}$, and $\vec{S}_1$, determining $\vec{S}_2$ and $\vec{P}$ is quite easy. The former is found via $\vec{S}_2 = \vec{J} - \vec{L} - \vec{S}_2$, and the latter is determined by making the following observations (i) P is a constant under the $S_{\text{eff}} \cdot L$ flow. So all we need to care about is the orientation of $\vec{P}$, which is dealt with in the next two bullet points. (ii) $\vec{L} = \vec{R} \times \vec{P}$; hence $\vec{L}$ is perpendicular to $\vec{R}$ and $\vec{P}$. (iii) under the $S_{\text{eff}} \cdot L$ flow, the azimuthal angle of $\vec{P}$ (around $\vec{L}$) changes by the same amount as that of $\vec{R}$. Bullets (ii) and (iii) let us determine the orientation of $\vec{P}$ using the orientation of $\vec{R}$. Note that the definitions and conventions of Ref. [19] do not totally align with those followed in this paper; so care has to be taken when merging the results of the two papers.

3. Solution for flow under J

As arrived at in Sec. VI B of Ref. [19], the effect of a flow under J by an amount $\Delta\lambda$ is increasing the azimuthal angles of $\vec{R}, \vec{P}, \vec{S}_1$, and $\vec{S}_2$ in the IF by an amount $\Delta\lambda$.

4. Solution for flow under L

As also arrived at in Sec. VI B of Ref. [19], the effect of a flow under L by an amount $\Delta\lambda$ is increasing the azimuthal angles of $\vec{R}$ and $\vec{P}$ in the NIF by an amount $\Delta\lambda$.

5. Solution for flow under J_z

As seen in Sec. VI B of Ref. [19], the effect of a flow under J_z by an amount $\Delta\lambda$ is increasing the azimuthal angles of $\vec{R}, \vec{P}, \vec{S}_1$, and $\vec{S}_2$ by an amount $\Delta\lambda$, around the z axis of any inertial frame. IF is a special inertial frame whose z axis coincides with $\vec{J}$.

APPENDIX B: THE BBHPNTOOLKIT PACKAGE

Here we give the details on some coded expressions in our BBHPNTOOLKIT package containing unnecessary higher PN order terms. Doing so does not increase the actual PN accuracy of our solutions since we never make use of the 2PN terms of the Hamiltonian. However doing so may bring the analytical solutions closer to the numerical solution (got by numerically integrating the 1.5PN EOMs):

(1) As mentioned already at the end of Sec. III D, we have kept more than necessary PN accuracy in Eq. (70) and by extension, Eq. (72). All the terms containing ϵ^q with $q \geq 2$ in Eq. (70) are unnecessary.

(2) The derivation of the solution Eqs. (12)–(30) of the mutual angles between the angular momenta for a flow under the Hamiltonian depends on the integration $\int dt/r^3$; see Eq. (3.6) of Ref. [17]. Here Newtonian r is enough for the desired level of accuracy, and Eqs. (12)–(30) have been derived using Newtonian r in $\int dt/r^3$. But in our BBHPNTOOLKIT, we have coded the results got by integrating 1.5PN accurate $1/r^3$. Equation (48) gives the 1.5PN-accurate r.

---

[1] B. Abbott *et al.* (LIGO Scientific and Virgo Collaborations), GWTC-1: A gravitational-wave transient catalog of compact binary mergers observed by LIGO and Virgo during the first and second observing runs, Phys. Rev. X **9**, 031040 (2019).

[2] R. Abbott *et al.* (LIGO Scientific and Virgo Collaborations), GWTC-2: Compact binary coalescences observed by LIGO and Virgo during the first half of the third observing run, Phys. Rev. X **11**, 021053 (2021).

[3] B. P. Abbott *et al.* (LIGO Scientific and Virgo Collaborations), GW170817: Observation of gravitational waves from a binary neutron star inspiral, Phys. Rev. Lett. **119**, 161101 (2017).

[4] L. Blanchet, Gravitational radiation from post-Newtonian sources and inspiralling compact binaries, Living Rev. Relativity **17**, 2 (2014).

[5] G. Schäfer and P. Jaranowski, Hamiltonian formulation of general relativity and post-Newtonian dynamics of compact binaries, Living Rev. Relativity **21**, 7 (2018).

[6] T. Damour and N. Deruelle, General relativistic celestial mechanics of binary systems. I. The post-Newtonian motion, Ann. Inst. Henri Poincaré Phys. Théor. **43**, 107 (1985), https://luth2.obspm.fr/IHP06/lectures/damour/DamourDeruelleAIHP85.pdf.

[7] B. M. Barker, S. N. Gupta, and R. D. Haracz, One-graviton exchange interaction of elementary particles, Phys. Rev. **149**, 1027 (1966).

[8] S. Tiwari, A. Gopakumar, M. Haney, and P. Hemantakumar, Ready-to-use Fourier domain templates for compact binaries inspiraling along moderately eccentric orbits, Phys. Rev. D **99**, 124008 (2019).

[9] M. Kesden, D. Gerosa, R. O'Shaughnessy, E. Berti, and U. Sperhake, Effective potentials and morphological transitions for binary black hole spin precession, Phys. Rev. Lett. **114**, 081103 (2015).

[10] D. Gerosa, M. Kesden, U. Sperhake, E. Berti, and R. O'Shaughnessy, Multi-timescale analysis of phase transitions in precessing black-hole binaries, Phys. Rev. D **92**, 064016 (2015).

[11] I. Hinder, L. E. Kidder, and H. P. Pfeiffer, Eccentric binary black hole inspiral-merger-ringdown gravitational waveform model from numerical relativity and post-Newtonian theory, Phys. Rev. D **98**, 044015 (2018).

[12] K. Chatziioannou, A. Klein, N. Yunes, and N. Cornish, Constructing gravitational waves from generic spin-precessing compact binary inspirals, Phys. Rev. D **95**, 104004 (2017).

[13] A. Klein and P. Jetzer, Spin effects in the phasing of gravitational waves from binaries on eccentric orbits, Phys. Rev. D **81**, 124001 (2010).

[14] A. Klein, Y. Boetzel, A. Gopakumar, P. Jetzer, and L. de Vittori, Fourier domain gravitational waveforms for precessing eccentric binaries, Phys. Rev. D **98**, 104043 (2018).

[15] C. Konigsdorffer and A. Gopakumar, Phasing of gravitational waves from inspiralling eccentric binaries at the third-and-a-half post-Newtonian order, Phys. Rev. D **73**, 124012 (2006).

[16] C. Konigsdorffer and A. Gopakumar, Post-Newtonian accurate parametric solution to the dynamics of spinning compact binaries in eccentric orbits: The leading order spin-orbit interaction, Phys. Rev. D **71**, 024039 (2005).

[17] G. Cho and H. M. Lee, Analytic Keplerian-type parametrization for general spinning compact binaries with leading order spin-orbit interactions, Phys. Rev. D **100**, 044046 (2019).

[18] S. Tanay, L. C. Stein, and J. T. Gálvez Ghersi, Integrability of eccentric, spinning black hole binaries up to second post-Newtonian order, Phys. Rev. D **103**, 064066 (2021).

[19] S. Tanay, L. C. Stein, and G. Cho, Action-angle variables of a binary black hole with arbitrary eccentricity, spins, and masses at 1.5 post-Newtonian order, Phys. Rev. D **107**, 103040 (2023).

[20] S. Tanay, Integrability and action-angle-based solution of the post-Newtonian BBH system (Lecture Notes), arXiv:2206.05799.

[21] https://github.com/sashwattanay/BBH-PN-Toolkit (2022).

[22] G. Cho and H. M. Lee, Analytic Keplerian-type parametrization for general spinning compact binaries with leading order spin-orbit interactions, Phys. Rev. D **100**, 044046 (2019).

[23] A. Fasano, S. Marmi, and B. Pelloni, *Analytical Mechanics: An Introduction*, Oxford Graduate Texts (OUP, Oxford, 2006).

[24] V. Arnold, K. Vogtmann, and A. Weinstein, *Mathematical Methods of Classical Mechanics*, Graduate Texts in Mathematics (Springer, New York, 2013).

[25] J. José and E. Saletan, *Classical Dynamics: A Contemporary Approach* (Cambridge University Press, Cambridge, England, 1998).

[26] A. Gopakumar and G. Schafer, Gravitational wave phasing for spinning compact binaries in inspiraling eccentric orbits, Phys. Rev. D **84**, 124007 (2011).

[27] H. Goldstein, C. Poole, and J. Safko, *Classical Mechanics* (Pearson, London, 2013).

[28] T. Damour and G. Schafer, Higher-order relativistic periastron advances and binary pulsars, Nuovo Cimento B **101,** 127 (1988).

[29] G. Cho, S. Tanay, A. Gopakumar, and H. M. Lee, Generalized quasi-Keplerian solution for eccentric, non-spinning compact binaries at 4PN order and the associated IMR waveform, Phys. Rev. D **105,** 064010 (2022).